



ELSEVIER

Journal of Membrane Science 105 (1995) 273–279

**Journal of  
MEMBRANE  
SCIENCE**

# Organic “template” approach to molecular sieving silica membranes

N.K. Raman<sup>a</sup>, C.J. Brinker<sup>b,\*</sup>

<sup>a</sup> *The UNM/NSF Center for Micro-Engineered Ceramics, University of New Mexico, Albuquerque, NM 87131, USA*

<sup>b</sup> *Sandia National Laboratories, Advanced Materials Laboratory, 1001 University Blvd. SE, Albuquerque, NM 87106, USA*

Received 28 December 1994; accepted 27 February 1995

## Abstract

We demonstrate a “template” approach to prepare microporous inorganic membranes exhibiting high flux combined with high selectivity, overcoming limitations inherent to both conventional inorganic (sol–gel, CVD) and organic membrane approaches. Hybrid organic–inorganic polymers prepared by co-polymerization of tetraethoxysilane (TEOS) and methyltriethoxysilane (MTES) were deposited on commercial asymmetric alumina supports. Heat treatments were employed to densify the inorganic matrix and pyrolyze the methyl ligands, creating a continuous network of micropores. Resulting membranes exhibited very high CO<sub>2</sub> permeance values ( $2.57 \times 10^{-3}$  cm<sup>3</sup>/cm<sup>2</sup> s cm Hg) combined with moderate CO<sub>2</sub>/CH<sub>4</sub> selectivities (12.2). Subsequent derivatization of the pore surfaces with monomeric TEOS significantly increased CO<sub>2</sub>/CH<sub>4</sub> separation factors (71.5) with only a modest reduction in CO<sub>2</sub> permeance ( $2.04 \times 10^{-4}$  cm<sup>3</sup>/cm<sup>2</sup> s cm Hg). Combined CO<sub>2</sub>/CH<sub>4</sub> selectivity factors and CO<sub>2</sub> fluxes exceeded those of all known organic membranes.

*Keywords:* Microporous and porous membranes; Gas separations; Organic templates

## 1. Introduction

Gas separation using membranes has evolved into a viable commercial technology for several industrially important gas separations such as dehydrogenation, CO<sub>2</sub>/CH<sub>4</sub>, and O<sub>2</sub>/N<sub>2</sub>. Membranes that separate CO<sub>2</sub> from CH<sub>4</sub> have potential applications in flue gas recovery, enhanced oil recovery, natural gas sweetening (CO<sub>2</sub> removal from high pressure methane in natural gas wells), and CO<sub>2</sub> recovery from land fills [1]. High solubility of CO<sub>2</sub> compared to CH<sub>4</sub> in several glassy organic polymers has made CO<sub>2</sub>/CH<sub>4</sub> separation using polymeric membranes economically attractive. How-

ever, several studies have shown that due to some intrinsic polymer property, such as free volume, there is an apparent trade-off between permeability and the selectivity independent of the chosen gas pair or the polymer [2]. For example, Robeson [3] in his extensive review of CO<sub>2</sub>/CH<sub>4</sub> separation factors in organic membranes, found an overall trend of decreasing separation factor with increasing permeability. In a plot of logarithm of separation factor and logarithm of permeability he defined an upper bound of combined separation factor and permeability achievable by organic membranes. In addition to this trade-off, another potential disadvantage of using organic polymer membranes for CO<sub>2</sub>/CH<sub>4</sub> separations is the strong chemical interaction between CO<sub>2</sub> and the organic polymers. CO<sub>2</sub> at high pressures can plasticize organic polymers thereby

\* Corresponding author. Tel: +1 505 272-7627, Fax: +1 505 272-7304.

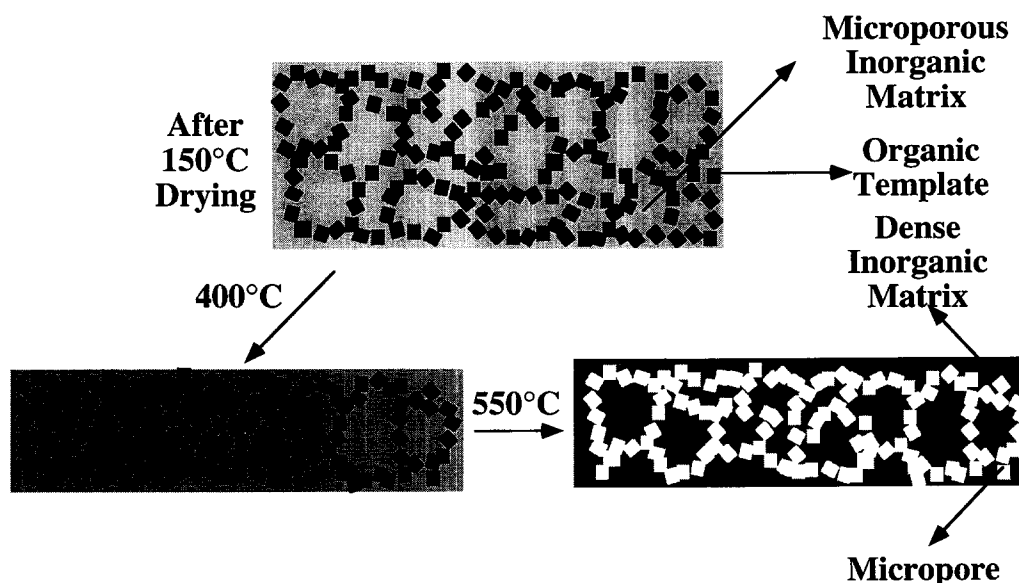


Fig. 1. Organic template approach showing the progressive densification of the inorganic matrix and creation of micropores by template removal during calcination.

significantly reducing membrane strength, integrity, and performance [4].

Porous inorganic membranes may overcome some of the inherent limitations of organic membranes, because there is no intrinsic relationship between permeability and selectivity. Permeability is controlled by the volume fraction porosity, whereas selectivity is determined by the pore size and pore size distribution. Another potential advantage of inorganic membranes is that they do not swell in high pressure  $\text{CO}_2$ . Unfortunately current procedures used to obtain the small pore sizes necessary for  $\text{CO}_2/\text{CH}_4$  separation rely upon promoting collapse of a gel network or making a virtually dense film by CVD, strategies that reduce membrane flux.

Here we describe a strategy for making inorganic membranes using fugitive organic ligands as micropore templates where we avoid this practical trade-off between permeability and selectivity (Fig. 1). Organic ligands embedded in a dense inorganic matrix are removed to create a continuous network of micropores. Ideally the organic ligand volume fraction is used to control porosity and hence flux, independently of selectivity, which depends on the ligand size and shape. In order to successfully implement this approach the following criteria must be satisfied: (1) the organic ligands must be uniformly incorporated in the inorganic

matrix without aggregation or phase separation to avoid creating pores larger than the size of the individual ligands; (2) the synthesis and processing conditions should result in a dense embedding matrix so that pores are created only by template removal; (3) template removal should be achieved without collapse of the matrix, so that the pores created preserve the original size and shape of the template; (4) after the first three criteria are satisfied, pore connectivity may be achieved by exceeding some percolation threshold of the organic ligands.

In this communication we demonstrate this template approach through synthesis of methyltriethoxysilane/tetraethoxysilane copolymers, processing into powders or supported membranes, thermal treatment to create microporous networks within dense inorganic matrices, and characterization by adsorption and transport measurements.

## 2. Experimental procedure

### 2.1. Materials

The chemicals used were obtained from the following sources: tetraethoxysilane (TEOS, Kodak, Rochester, NY); methyltriethoxysilane (MTES, Hüls,

Bristol, PA); absolute ethanol (EtOH, Midwest Grain, Pekin, IL); 1 M hydrochloric acid (HCl, J.T. Baker, Phillipsburg, NJ). All chemicals were used as received without further purification.

## 2.2. Sol and bulk gel preparation

Sols were prepared by co-polymerization of methyltriethoxysilane and tetraethoxysilane using a two step acid-catalyzed process [5]<sup>1</sup>. In the first step MTES, TEOS, EtOH, H<sub>2</sub>O, and 1 M HCl with molar ratios  $x:1-x:3.8:1.1:7.0 \times 10^{-4}$ , where  $x$  ranged from 10 to 55 mol%, were refluxed at 60°C for 90 min with stirring at 200 rpm. In the second step additional water and 1 M HCl were added at room temperature resulting in the final molar ratio of  $x:1-x:3.8:5.1:0.056$ . The sols were aged at 50°C for a  $t/t_{\text{gel}}=0.24$  and diluted 1:2 with ethanol (volume sol:volume EtOH) to obtain a sol suitable for coating. Xerogel (dry gel) bulk samples for gas adsorption measurements were prepared by gelling undiluted sols at 50°C followed by drying (50°C) and grinding using a mortar and pestle. The powders were calcined in air at a heating and cooling rate of 1°C/min to 150, 400, or 550°C and held at the respective temperatures for 30 min.

Dilatometry specimens were prepared by casting undiluted sols in cylindrical molds (diameter = 0.78 cm and length = 5 cm), followed by gelation and aging for 3 days at 50°C under sealed conditions. The gel rods were then inserted into 22 × 175 mm glass tubes and dried at 50°C for 5 days followed by heating to 150°C at a heating rate of 6°C/h and holding isothermally for 6 h.

## 2.3. Membrane deposition

Membranes were deposited on commercial Membralox<sup>®</sup> supports (supplied by U.S. Filter in 25 cm lengths) that were cut into 5 cm sections using a diamond wafering saw and cleaned using a CO<sub>2</sub> SNO-GUN<sup>™</sup> cleaner. Each uncoated support was pre-calcined to 400 or 550°C according to the final heat treatment of the silica membrane to be deposited. The calcined supports were outgassed in flowing ultra-high purity N<sub>2</sub> at 150 or 400°C for 6 h before membrane deposition. Membranes were deposited using a

Compumotor<sup>™</sup> linear translation stage in a dry box with nitrogen ambient. The support was dip-coated at a constant immersion and removal rate of 20 cm/min. The support was held immersed in the sol for 100 s before removal. The dip-coated membrane was then dried under N<sub>2</sub> ambient for 15 min, before calcination in air to 150, 400 for 0.5 h or 550°C for 4 h with a heating and cooling rate of 1°C/min. The dip-coated membranes were outgassed at 150 or 400°C for 6 h in flowing ultra-high purity N<sub>2</sub> prior to transport measurements.

Pore surfaces of the single layer membranes were derivatized by successive reaction with a solution of neat (unhydrolyzed) TEOS that was diluted 1:12 with EtOH (volume TEOS:volume EtOH), allowing monolayer by monolayer “tuning” of pore size. The dip-coating procedure and the calcination treatment were very similar to that used for the first coating.

## 2.4. Thermal analysis

TGA/DTA experiments were performed using a Polymer Labs STA 1500 instrument in flowing air with a heating rate of 10°C/min to 1000°C on samples that were prepared by fast drying 2–3 ml of the sol in an open glass Petri dish at 150°C.

## 2.5. Structural characterization

An ASAP 2000 (Micromeritics, Norcross, GA) instrument was used to measure N<sub>2</sub> sorption isotherms of the bulk xerogels after outgassing at 150 or 250°C for 12 h at 0.01 Torr. The apparent surface area (m<sup>2</sup>/g) was calculated from the BET equation [6] using N<sub>2</sub> molecular cross sectional area = 0.162 nm<sup>2</sup> and the linear region between  $0.05 \leq P/P_0 \leq 0.20$  that gave a least square correlation coefficient  $R^2 > 0.9999$  for at least 4 adsorption points. The pore volume (cm<sup>3</sup>/g) was calculated from the high  $P/P_0$  portion of the isotherm where the volume of N<sub>2</sub> adsorbed was constant.

A Netzsch differential dilatometer (Gerätebau, Selb, Germany) was used to measure the linear shrinkage of bulk xerogel specimens during densification. A  $5 \pm 0.25$  mm gel rod combined with a 20 mm piece of  $\alpha$ -alumina was mounted in the system so that the final length of the sample was 25 mm. A 25 mm  $\alpha$ -Al<sub>2</sub>O<sub>3</sub> rod was used as a reference. The gels were heated in air to 800°C at 0.2°C/min.

<sup>1</sup> <sup>29</sup>Si NMR shows uniform incorporation of organic templates.

Transmission electron microscopy (TEM) of the samples was performed to determine thickness and morphology of the membrane layer. Broken fragments of the membrane/support structure were sectioned with a diamond wafering saw, ground and polished to a thickness of 1  $\mu\text{m}$ , and ion milled to a thickness of several hundred angstroms. TEM was performed using a Philips Model CM-30 300 KV analytical instrument equipped with a LINK EDS analyzer.

### 2.6. Transport measurements

Single gas permeabilities of the uncoated supports and supported membranes were measured at 25°C as a function of pressure (20–80 psig) using the series of gases: He, N<sub>2</sub>, CO<sub>2</sub>, CH<sub>4</sub>, and SF<sub>6</sub>. The tubular membrane was mounted in a gas flow cell, in such a fashion that compression of viton gasket material at the ends of the membrane prevented bypassing [7]. Compressed gas was flowed into the annulus of the tubular support, with the flow rate set using a mass flow controller or a bubble flow meter. The pressure drop across the membrane was measured using pressure gauges, and the average pressure across the membrane could be varied using a valve downstream from the flow cell. The permeability measurements were conducted by measuring the pressure on both sides of the membrane as a function of the steady-state mass flow rate permeating the membrane. The separation factor was calculated by taking the ratio of the permeance of the individual gases.

## 3. Results and discussion

### 3.1. Structural characterization of bulk xerogels

N<sub>2</sub> sorption isotherms of the 10 mol% MTES/TEOS xerogels as a function of the calcination temperature are shown in Fig. 2 along with a partial CO<sub>2</sub> isotherm of the 550°C sample. The N<sub>2</sub> sorption isotherms appear to change from Type I, characteristic of microporous materials at 150°C and 400°C respectively to Type II, characteristic of non-porous materials after calcination at 550°C. However the partial CO<sub>2</sub> isotherm shows the

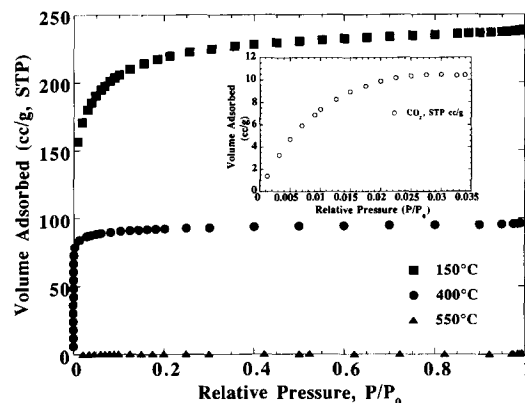


Fig. 2. N<sub>2</sub> adsorption isotherms of the 10 mol% MTES/TEOS xerogels as a function of calcination temperature. Inset shows the partial CO<sub>2</sub> isotherm of the 550°C calcined sample.

550°C sample also to be microporous (see inset in Fig. 2)<sup>2</sup>.

The linear shrinkage of the 10 mol% MTES/TEOS xerogels versus temperature along with the corresponding weight loss measured by TGA is shown in Fig. 3. The combined results from sorption, shrinkage and weight loss experiments are consistent with a progressive densification of the microporous inorganic matrix over the 150–550°C temperature range. Up to about 350°C shrinkage is proportional to weight loss suggesting that densification occurs mainly due to continued condensation reactions that expel water from the gel network. Above 350°C shrinkage and weight loss are not well-correlated. Shrinkage occurs by sintering accompanied by condensation reactions. Compared to

<sup>2</sup> The apparent discrepancy between the N<sub>2</sub> and CO<sub>2</sub> data arises because the pores in the xerogel are so small that the diffusion of N<sub>2</sub> at 77 K is severely kinetically limited compared to CO<sub>2</sub> at 273 K [5].

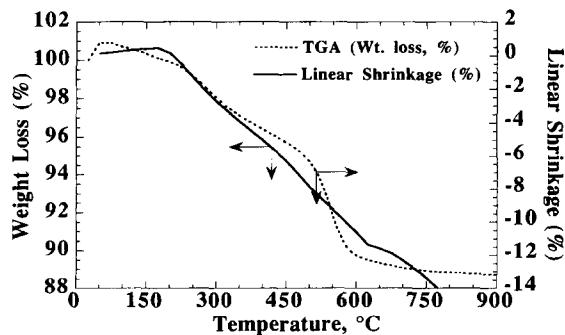


Fig. 3. Linear shrinkage and weight loss of the 10 mol% MTES/TEOS xerogels versus temperature.



Fig. 4. Cross-sectional TEM image of 550°C calcined 10 mol% MTES/TEOS membrane layer deposited on a U.S. Filter®  $\gamma$ -Al<sub>2</sub>O<sub>3</sub> membrane support. Region A indicates the  $\gamma$ -Al<sub>2</sub>O<sub>3</sub> support (pore size = 4.0 nm). Region B is the external microporous SiO<sub>2</sub> layer.

conventional sol-gel silica, sintering is enhanced due to the lower connectivity of the siloxane network imposed by inclusion of the non-hydrolyzable methyl

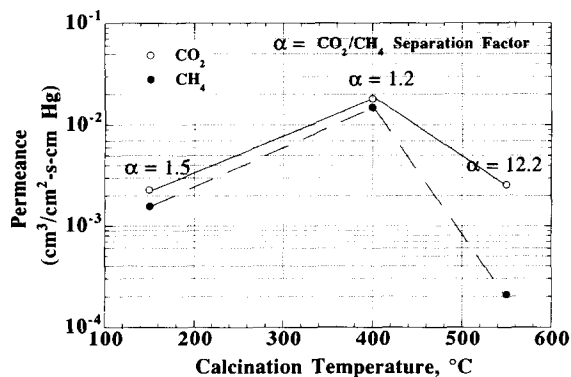


Fig. 5. CO<sub>2</sub> and CH<sub>4</sub> permeance of the 10 mol% MTES/TEOS membranes as a function of calcination temperature. The line is a visual guide.

ligands. The sharp weight loss occurring between about 450 and 600°C is attributed primarily to the oxidative pyrolysis of methyl ligands and any residual ethoxy ligands (the Corresponding DTA results showed a broad exotherm extending from about 350 to 800°C). The absence of a corresponding enhancement of the extent of shrinkage over this temperature range is consistent with the creation of porosity. By 550°C, the scale of the porosity is apparently quite small and the densification of the inorganic matrix is virtually complete based on essentially zero uptake of N<sub>2</sub> at 77 K versus CO<sub>2</sub> at 273 K. In summary these results are qualitatively consistent with the template approach portrayed in Fig. 1.

### 3.2. Structural characterization of membranes

Cross-sectional TEM at magnifications of  $450 \times 10^3$  and  $1 \times 10^6$  showed the membrane layer deposited on

Table 1

Summary of the permeances ( $\text{cm}^3/\text{cm}^2 \text{ s cm Hg}$ ) and the separation factors ( $\alpha$ ) of the 10 and 40 mol% MTES/TEOS membranes before and after surface derivatization

Membrane	Time (h) at temperature ( $^{\circ}\text{C}$ )	He permeance	$\alpha_{\text{He}/\text{SF}_6}$	$\alpha_{\text{He}/\text{N}_2}$	$\text{CO}_2$ permeance	$\alpha_{\text{CO}_2/\text{CH}_4}$
10% MTES/TEOS $t/t_{\text{gel}}=0.24$	0.5 at 150	$2.55 \times 10^{-3}$	12.1	8.7	$2.29 \times 10^{-3}$	1.5
	0.5 at 400	$2.24 \times 10^{-2}$	7.2	1.3	$1.81 \times 10^{-2}$	1.2
	4.0 at 550	$2.31 \times 10^{-3}$	24.3	15.4	$2.57 \times 10^{-3}$	12.2
Surface derivatization with 1:12 TEOS monomer	4.0 at 400	$1.32 \times 10^{-4}$	328	14.4	$2.04 \times 10^{-4}$	71.5
40% MTES/TEOS $t/t_{\text{gel}}=0.24$	0.5 at 150	$1.34 \times 10^{-3}$	12.0	2.2	$1.72 \times 10^{-3}$	1.8
	0.5 at 400	$2.71 \times 10^{-3}$	15.2	2.2	$3.29 \times 10^{-3}$	2.0
	4.0 at 550	$4.64 \times 10^{-3}$	14.3	2.4	$6.79 \times 10^{-3}$	3.2
Surface derivatization with 1:12 TEOS monomer	4.0 at 400	$2.00 \times 10^{-4}$	47.6	7.7	$5.0 \times 10^{-4}$	36.5

the  $\gamma\text{-Al}_2\text{O}_3$  supports to be featureless and crack free under the deposition conditions (see Fig. 4). The thickness of the external membrane layer measured from the TEM micrographs varied between 375 to 1130 Å from one region of the sample to the other. We attribute this to the non-uniform thickness and/or the surface roughness of the 40 Å  $\gamma$ -alumina support [7]. The EDS analysis revealed that silica penetrated the support uniformly to a depth of about 2  $\mu\text{m}$ .

### 3.3. Transport characterization of membranes

Permeance data of corresponding membranes are shown in Fig. 5. Thin films show somewhat different

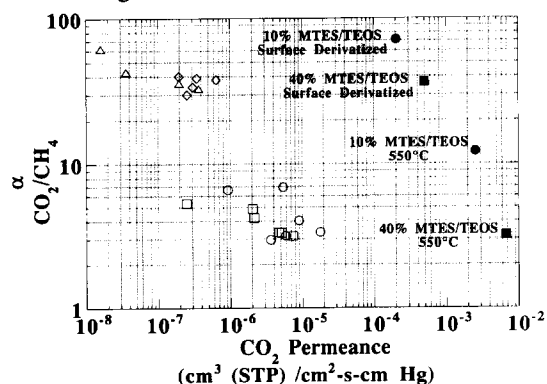


Fig. 6. Comparison of  $\text{CO}_2$  permeance and  $\text{CO}_2/\text{CH}_4$  separation factors of known organic membranes and those of microporous inorganic membranes prepared in this study:  $\circ$ , silicone polymers with different side chains [10];  $\square$ , silicone polymers with different backbones [10];  $\diamond$ , polyamide homo- and co-polymers [11];  $\triangle$ , PMDA sequence of polyamides [12];  $\bullet$ , 10 mol% MTES/TEOS membranes; and  $\blacksquare$ , 40 mol% MTES/TEOS membranes. Permeances calculated from the average thickness data of the membranes reported in the literature.

behavior than expected from the sorption studies performed on bulk samples, i.e. permeability initially increases with heating due to partial pyrolysis of organic ligands then decreases due to sintering. Presumably the constraint imposed by the underlying support retards the sintering kinetics [8] so that for membranes substantial densification of the inorganic matrix occurs only above 400°C. As shown in Fig. 5 both the  $\text{CO}_2$  and the  $\text{CH}_4$  permeance of the 10 mol% MTES/TEOS membranes increased while the  $\text{CO}_2/\text{CH}_4$  separation factor decreased somewhat after calcination at 400°C for 0.5 h. However after calcination at 550°C for 4 h the permeance of all the gases decreased dramatically compared to  $\text{CO}_2$  and He. The separation factors for the gas pairs,  $\text{CO}_2/\text{CH}_4$ , He/ $\text{N}_2$ , and He/ $\text{SF}_6$  (12.2, 15.4, 24.3, respectively) are well above the ideal Knudsen values and increase as the difference in their kinetic diameters increases, implying that a molecular sieving mechanism governs transport (see Table 1). The  $\text{CO}_2$  and He permeance of the membranes after calcination at 550°C were in general higher than those measured after drying at 150°C, indicating a net creation of porosity by this approach. In addition, the permeance values of the 40 mol% MTES/TEOS membranes exceed those of 10 mol% MTES/TEOS membranes showing that flux is at least partially controlled by the volume fraction of template addition. Overall we infer from these results that densification of the matrix combined with the removal of template ligands creates microporous channels within a dense inorganic framework. The pores created are of molecular dimension as evidenced by separation factors

exceeding ideal Knudsen values. The efficacy of this approach is apparent when we compare the results for MTES/TEOS membranes with known organic polymer membranes in Fig. 6. For a selectivity factor of 12 this approach results in over four orders of magnitude improvement in permeance compared to organic polymer membranes.

The transport behavior of the MTES/TEOS membranes exhibiting high permeance and moderate selectivities can be “fine-tuned” using surface derivatization techniques in which pore size is reduced in a monolayer-by-monolayer fashion [9]. After surface derivatization and calcination at 400°C for 4 h the He/SF<sub>6</sub>, He/N<sub>2</sub>, and CO<sub>2</sub>/CH<sub>4</sub> separation factors were 328, 14.4, and 71.5 respectively, for 10 mol% MTES/TEOS membranes. The corresponding separation factors for the 40 mol% MTES/TEOS membranes were 47.6, 7.7, and 36.5 respectively. It is noteworthy that, compared to organic membranes exhibiting separation factors in the 70–80 range, the microporous inorganic membranes exhibit more than 1000× greater permeance (see Fig. 6).

#### 4. Conclusions

We have demonstrated an organic template strategy that allows formation of inorganic membranes exhibiting high permeability combined with high selectivity. This approach is obviously not limited to CO<sub>2</sub>/CH<sub>4</sub> separation: it has broad applicability in the general area of microporous membranes. For the specific case of CO<sub>2</sub>/CH<sub>4</sub> separations, we have demonstrated combined flux and selectivity superior to those of known organic membranes but, with the added advantage, that the inorganic framework should be non-swella-

ble. This work was supported by the Gas Research Institute, the Department of Energy –Morgantown Energy Technology Center. In addition, we are grateful to T.J. Headley of Sandia National laboratories for the TEM sample preparation and analysis. Sandia National laboratories is a U.S. Department of Energy facility supported by DOE Contract Number DE-AC04-76-DP00789.

#### References

- [1] J.M.S. Henis, in D.R. Paul and Y.P. Yampol'skii (Eds.), *Polymeric Gas Separation Membranes*, CRC Press, MA, 1994, pp. 157.
- [2] N. Platé and Y.P. Yampol'skii, in D.R. Paul and Y.P. Yampol'skii (Eds.), *Polymeric Gas Separation Membranes*, CRC Press, MA, 1994, pp. 157.
- [3] Lloyd M. Robeson, Correlation of separation factor versus permeability for polymeric membranes, *J. Membrane Sci.*, 62 (1991) 165–185.
- [4] M.R. Pixton and D.R. Paul, in D.R. Paul and Y.P. Yampol'skii (Eds.), *Polymeric Gas Separation Membranes*, CRC Press, MA, 1994, pp. 157.
- [5] C.J. Brinker and G.W. Scherer, *Sol–Gel Science*, Academic Press, San Diego, CA, 1990, pp. 560–562.
- [6] S.J. Gregg and K.S.W. Sing, *Adsorption, Surface area and Porosity*, 2nd ed., Academic Press, New York, 1982.
- [7] C.J. Brinker, T.L. Ward, R. Sehgal, N.K. Raman, S.L. Hietala, D.M. Smith, D.-W. Hua and T.J. Headley, “Ultramicroporous” silica-based supported inorganic membranes, *J. Membrane Sci.*, 77 (1993) 165–179.
- [8] T.J. Garino and H.K. Bowen, Kinetics of constrained-film sintering, *J. Am. Ceram. Soc.*, 73(2) (1990) 251–257.
- [9] N.K. Raman, T.L. Ward, C.J. Brinker, R. Sehgal, D.M. Smith, Z. Duan, M. Hampden-Smith, J.K. Bailey and T.J. Headley, Catalyst dispersion on supported ultramicroporous inorganic membranes using derivatized silylation agents, *Appl. Catal. A, General*, 69 (1993) 65–82.
- [10] S.A. Stern, V.M. Shah and B.J. Hardy, Structure–permeability relationships in silicone polymers, *J. Polym. Sci., Part B: Polym. Phys.*, 25 (1987) 1263–1298.
- [11] G. Zoia, S.A. Stern, A.K. ST. Clair and J.R. Pratt, Permeability relationships in polyimide copolymers, *J. Polym. Sci., Part B: Polym. Phys.*, 32 (1994) 53–58.
- [12] S.A. Stern, Y. Mi and H. Yamamoto, Structure/permeability relationships of polyimide membranes. Applications to the separation of gas mixtures, *J. Polym. Sci., Part B: Polym. Phys.*, 27 (1989) 1887–1909.

#### Acknowledgements

Portions of this work were supported by the Electric Power Research Institute, the National Science Foun-